

Experimental Realization and Synchronization of a Chua Circuit

Daniella Masante. Department of Physics. University of California, Davis.
Physics Building, 1 Shields Avenue, Davis, CA 95616 USA. masante@ucdavis.edu

Abstract

A Chua circuit, known to exhibit chaotic behavior, has been constructed and studied. The circuit was built with a potentiometer as a control resistor, and chaotic dynamics such as limit cycles and attractors were measured and compared to a numerical simulation. The circuit showed intermittent chaos from 1307Ω to 1777Ω , and were in agreement with the numerical simulation within an 11.81% to 18.81% relative error range. Two Chua Circuits were then successfully synchronized using the bidirectional method.

However, they had trouble implementing the multiplications that appear on the equations of motion, so their circuit ended up being very complex.

After almost three years of work, the circuit was finally completed in October 1983. Unfortunately, the premier was a spectacular disaster due to the failure of one of the integrated circuits [3]. It was then when Leon Chua, a visiting professor at the time, wondered if one could construct a circuit that would not be governed by the Lorentz equations, but would still give rise to chaotic behavior.

1. Introduction

This work was motivated by the question “Can you synchronize chaos?” which was made by me during PHY256A. The physical implementation of a chaotic system was motivated by section 9.5 “Using Chaos to Send Secret Messages” of the book *Nonlinear Dynamics and Chaos* by Steven H. Strogatz. In this particular section, a brief discussion on how to construct a chaotic mask using an electronic implementation of the Lorentz equations is held. A Chua Circuit was then preferred over the Lorentz both for simplicity and historical reasons.

When Edward Lorentz provided his idealized model of the atmosphere [1], some scientists questioned the physical nature of his result. Their argument was that no real experimental confirmation could ever be made because his model was very crude and simplified; that his model could only be exhibited by abstract mathematical models but had no connection to reality.

In order to settle the ongoing dispute, Takashi Matsumoto’s research group decided to build an electrical circuit that would mimic the equations [2].

The Chua circuit was born after he figured out exactly how to remove all the unnecessary components of the Lorentz circuit while still preserving the chaos, and Chua himself was among the first persons who showed that chaos can be easily constructed and observed.

The first goal of this work was to build a Chua circuit with a variable resistor as a bifurcation parameter. Secondly, a numerical simulation was used to compare the experimental measurements. The measurements were compared both visually and in terms of the variable resistor. Lastly, two Chua circuits were synchronized using the bidirectional synchronization method discussed on the already mentioned Strogatz book.

Section 2 on this work introduces the Chua circuit. In section 3 a fixed point analysis is performed on the equations of motion of the Chua circuit. Section 4 details the experimental realization of the Chua circuit. Section 5 goes through the numerical simulation methodology and parameters. In section 6 all of the results are presented and a discussion of them is done on section 7. Finally, the conclusions and a brief proposal of future work are discussed in section 8.

2. Background

Back when he was figuring out how to create his circuit, Leon Chua had a lot of decisions to make. He intuitively knew that his circuit didn't have to be as complicated as the Lorentz prototype to get chaos. However, he also knew going into his search that he needed to reach a certain minimal complexity (Poincaré-Bendixson theorem) of at least three degrees of freedom to not lose the behavior [4].

That was the first question that Leon Chua had to ask himself: what is a degree of freedom on an electrical circuit? If the system contained only resistive components all currents and voltages could be computed directly, without any additional knowledge. If the information about this current is provided, it can be treated just like an ordinary current source and the resulting resistive equations can be solved. Therefore, such system would have zero degrees of freedom.

The answer is that a degree of freedom is any component in which the relation between voltage and current depends on previous history (i.e. a differential relation). This is the case because the number of degrees of freedom describes how many scalar quantities (at each moment in time) are needed to fully classify the state of the circuit, meaning that every voltage and current can be computed from such information. This is achievable by energy-carrying components, such as inductors or capacitors. And it also meant that by default Chua's final circuit would be autonomous, which means dependent on time. So Chua decided to use one of the former and two of the later and moved on.

The second problem that Chua encountered is that a linear system cannot exhibit chaotic behavior [5]. He knew that he needed a non-linear component because a linear system is independent of scale and therefore whatever happens on a small scale happens at a larger scale; there is no element of surprise on a linear system. Chua opted for a purely resistive non-linear component, but that didn't reduce his list of possibilities a great much. He explored a lot of possibilities with elements such as transistors, varistors, diodes and many more to see what worked best. At the end he decided to use operational amplifiers, and the first version of the Chua Diode was born.

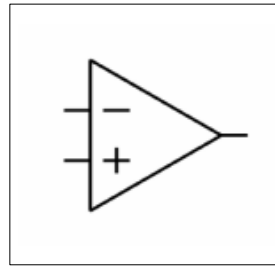


Figure 1- Schematic representation of an ideal operational amplifier

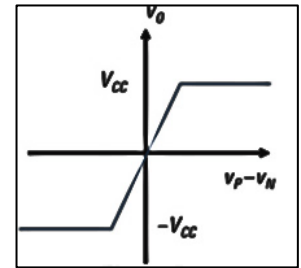


Figure 2- Operational Amplifier characteristics between voltage difference and amplified voltage

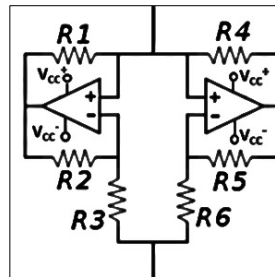


Figure 3- Schematic representation of a Chua diode

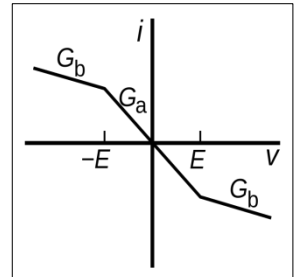


Figure 4- Ideal voltage/current relationship for a Chua diode

“The rather surprising fact first proven by Chua, known as the Global Unfolding Theorem, is that a circuit satisfying these three criteria (autonomous, three energy storing components and the only nonlinear devices are operational amplifiers) either contains more operational amplifiers than minimally needed for chaos or is conjugate to family of circuits of the Chua-Kennedy. Hence the Global Unfolding Theorem provides mathematical rigor to the statement that the Chua circuit is “the simplest chaotic circuit” and motivate its use as a model system for chaotic systems.” [3]

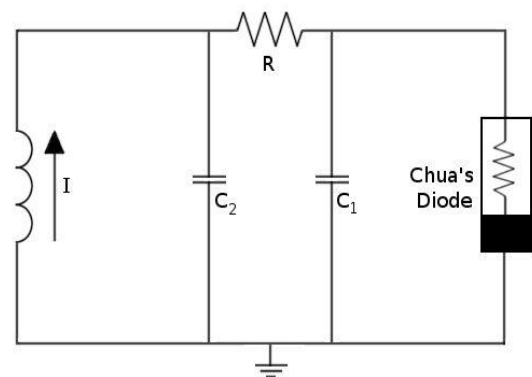


Figure 5- Chua circuit

3. Dynamical System

The three equations of motion for the circuit are given by:

$$\begin{aligned} \frac{dV_1}{dt} &= \left[\frac{1}{RC_1} \right] ((V_2 - V_1) - R * g(v_1)) \\ \frac{dV_2}{dt} &= \left[\frac{1}{RC_2} \right] ((V_1 - V_2) - R * i_L) \\ \frac{di_L}{dt} &= \left[\frac{1}{L} \right] (-v_2) - R_L i_L \end{aligned}$$

Where $g(v_1)$ is the Chua diode. In these equations the state variables V_1 and V_2 are the voltages across the capacitors, C_1 and C_2 , i_L is the current flowing through the inductor L , which has an internal resistance R_L .

There are three fixed points to these equations, which are:

$$p_0 = [0, 0, 0]$$

$$p_{1,2} = \pm \left[\frac{-E(G_b - G_a)(r_L + R)}{1 + (R + r_L)G_b}, \frac{-E(G_b - G_a)(r_L)}{1 + (R + r_L)G_b}, \frac{+E(G_b - G_a)(r_L)}{1 + (R + r_L)G_b} \right]$$

Where G_a and G_b are the slopes of the Chua diode (see figure 4). In these equations the state variables v_1 and v_2 are the voltages across the capacitors, C_1 and C_2 , i_L is the current flowing through the inductor L , which has an internal resistance R_0 .

The fixed points p_1 and p_2 are only feasible if $V_1 \geq E$ and $V_1 \leq -E$ respectively, leading to the following condition:

$$\frac{E(-G_a + G_b)(GR_L + 1)}{\frac{1}{R} + \frac{G_b R_L}{R} + G_b} \geq E$$

Rewriting this condition gives a lower and upper bound on the variable resistor R :

$$\left| \frac{G_b}{1 + G_b R_L} \right| \leq \frac{1}{R} \leq |G_a|$$

Performing a stability analysis [6] concludes that p_0 is always an unstable equilibrium point, while there is a region where the real part of all three eigenvalues is negative for p_1 and p_2 . The crossing of the imaginary axis is what determines the stable region for the parameter R .

There is also a resistance value at which a Hopf bifurcation appears [7], at which point the equilibrium point loses its stability and a stable limit cycle appears.

4. Experimental Setup

4.1 Experimental Realization

Figure 6 shows the schematic representation of the electric circuit assembled for this work.

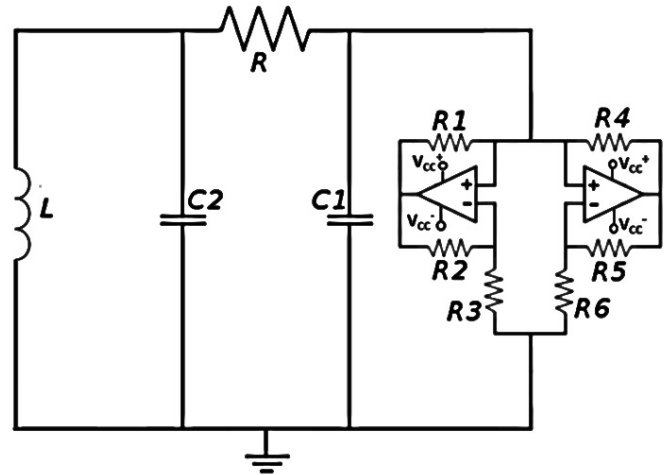


Figure 6- Circuit diagram of Chua circuit used in experiments

Where $R_1 = 220 [\Omega]$, $R_2 = 220 [\Omega]$, $R_3 = 2.2 [k\Omega]$, $R_4 = 22 [k\Omega]$, $R_5 = 22 [k\Omega]$, $R_6 = 3.3 [k\Omega]$, $C_1 = 10 [nF]$, $C_2 = 100 [nF]$, $L = 18 [mH]$, $R_L = 13 [\Omega]$ and R is a potentiometer.

4.2 The Chua Diode

The diode's characteristic behavior is derived by studying each section containing an operational amplifier independently. In figure 3 two of those sections can be seen connected in parallel. These sections are known as negative impedance converters, and they effectively behave as a resistor that creates energy instead of dissipating it, as long as the voltage is within the linear range of the operational amplifier [3].

Once the voltage is beyond this range, the differential resistance becomes positive, as in an ordinary resistor, meaning that the total component behaves like a piecewise linear device. A circuit with only one of these devices is not enough to get chaos, as such a circuit will reach a stable equilibrium due to energy dissipation.

However, if two of these devices are connected in parallel, the total current created will be the sum of both devices and the resulting voltage vs. current characteristics will have five linear sections, with the possibility for the three inner sections to all have negative differential resistance [8]. This is exactly what was obtained in figure 7.

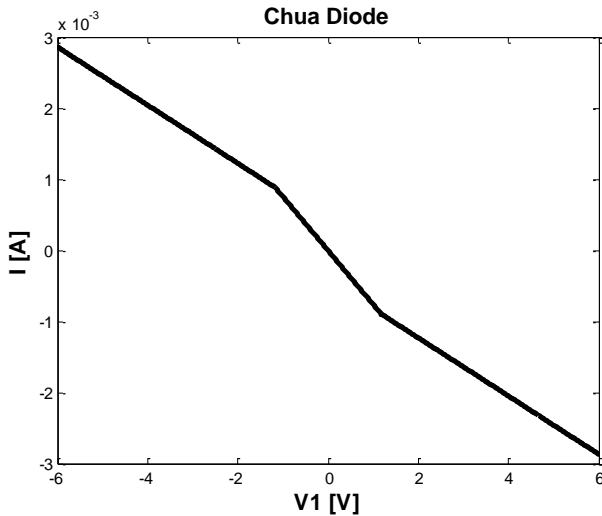


Figure 7- Numerically obtained voltage/current relationship for the Chua diode used on this work.

4.3 List of Materials

Table 1 contains a list of materials used to realize the circuit.

Device	Stock Code	Qty	Description
Capacitor	Mapln Sc Series	2	Metallized Polyester Film (MKT) Capacitors
Inductor	PCH45X186KLT	1	Axial Lead Power Choke
Resistor	TOPCOFRLD008	6	Metal Film full range resistor
Potentiometer	B01LYHMKNN	1	Logarithmic Dual Rotary Potentiometer
Operational Amplifier	Tl6PCSUA741CP	2	General Purpose Operational Amplifier

Table 1- List of materials. All elements are Rohs compliant

Resistors- Metal firm resistors with 1% tolerance were used, as they have low noise and weak nonlinearity.

Capacitors- To achieve a sharp image, metallized polyester capacitors were selected. Their leakage resistance was measured and deemed unimportant.

Inductor- The general recommendation in the literature is to use a gyrator circuit in favor of a physical coil. Of the criticism raised in the literature against the inductor, the most serious one is the claim of non-linearity due to hysteresis. The inductor also needs to have an internal resistance lower than 30[Ω]. These specifications make it hard to find a suitable physical inductor and thus the gyrator is preferred. However, a series of inductor that comfortably met the criteria was found and thus an actual inductor was used on this experimental setup.

Figure 8 shows the physical realization of the Chua circuit.

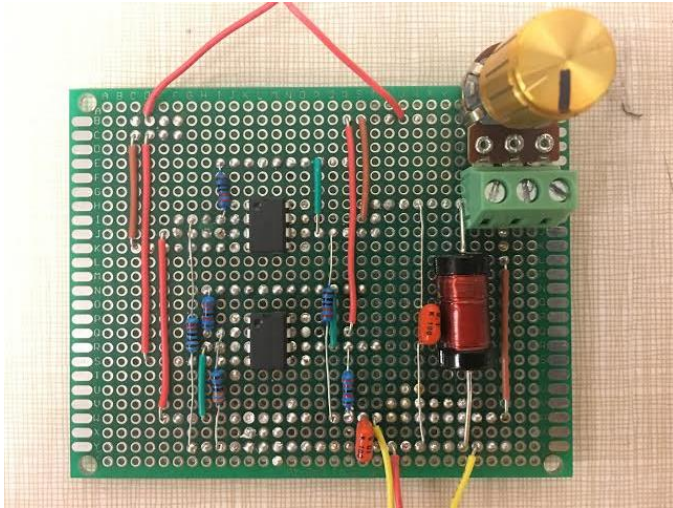


Figure 8- Chua circuit

The greatest disadvantage of the setup is that it is not possible to choose initial conditions. The setup is initialized when the voltage supply of the operational amplifiers is turned on. Although the initial conditions are random and unknown, polarity ensures that the voltage across capacitor C1 is negative. Therefore the initial conditions are always negative.

4.4 Synchronization- Bidirectional Chua Circuit

There are many ways to couple a system for synchronization, the two most popular are bidirectional, and Master/Slave (unidirectional). This work briefly explored the bidirectional approach.

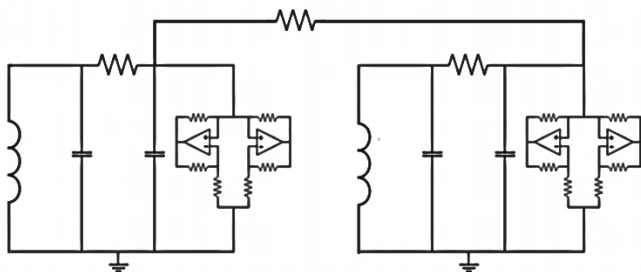


Figure 9- Bidirectional Chua circuit. All of the component values were replicated. A 1[k Ω] resistor was used as synchronization resistor.

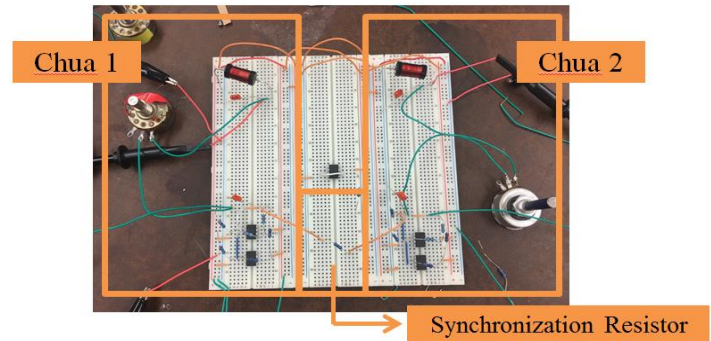


Figure 10- Experimental realization of the bidirectional Chua circuit.

5. Numerical Setup

In order to validate the experimental results, a numerical simulation was elaborated on Sage Math.

While a dimensionless model is what is most commonly used and referred to in academic literature, this work used a realistic model in which all of the component values were used. The objective of this was to preserve the resistor value at which every solution was taken in order to compare it to the experimental obtained one.

A finite difference method, with a timestep of 0.0000001 seconds. The number of iterations used was 100000, and the first 10% of them were discarded as transient behavior was not important on this work.

A swipe of integer values of R was done going down from 2500[Ω], with five different aleatory and negative initial conditions for each value.

6. Results

6.1 Numerical Predictions vs. Experimental Results

If the resistance is chosen to be a very high value, any oscillations will quickly be dissipated, and the system will after a transient simply be in an equilibrium state with a steady current flowing through the resistor and constant voltages.

This means that the circuit effectively behaves as if the left part was replaced by a resistor. It also means that it is easier to analyze the behavior of the circuit by decreasing the resistance, rather than increasing it, which is what was done on this work.

As the resistance is decreased, the equilibrium point must sooner or later be unstable, as the dissipation is no longer enough to quell any disturbances that appear. Instead, such a perturbation causes a self-oscillatory cycle where the left part of the circuit is charged and then discharged.

This is the Hopf bifurcation, which was first reached at 2015 $[\Omega]$ on the numerical prediction and 1777 $[\Omega]$ on the experiment.

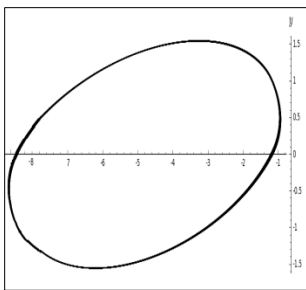


Figure 11- Numerical prediction for the original limit cycle.
R= 2015 $[\Omega]$

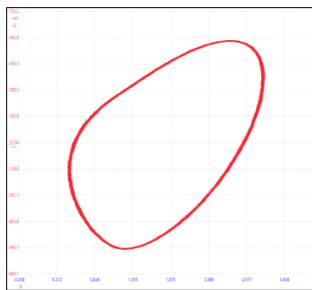


Figure 12- Experimental result for the original limit cycle.
R= 1777 $[\Omega]$

As the resistance is further decreased, this limit cycle also becomes unstable, since a small deviation in entry will cause the trajectory to “overshoot” the correct exit point, causing the next cycle that follows to undershoot instead [3]. Hence a limit cycle of twice the period is formed by this cycle of over- and undershooting of the original limit cycle (since the system now must transverse two loops before returning to the initial configuration). The first period doubling for the single scroll was observed at 2001 $[\Omega]$ on the numerical prediction and 1714 $[\Omega]$ on the experiment.

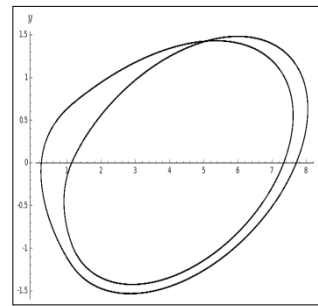


Figure 13- Numerical prediction for the first period doubling.
R= 2001 $[\Omega]$

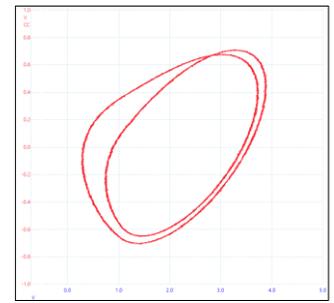


Figure 14- Experimental result for the first period doubling.
R= 1714 $[\Omega]$

Further decrease of the resistance causes a further doubling in period time by the same mechanism. The second period doubling for the single scroll was observed at 1998 $[\Omega]$ on the numerical prediction and 1701 $[\Omega]$ on the experiment.

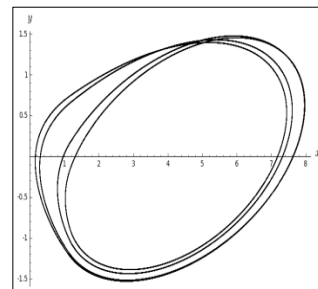


Figure 15- Numerical prediction for the second period doubling.
R= 1998 $[\Omega]$

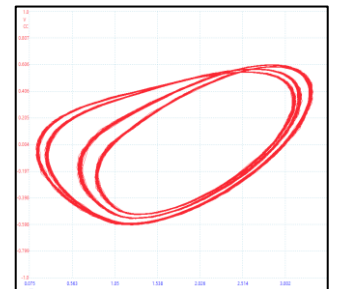


Figure 16- Experimental result for the second period doubling.
R= 1701 $[\Omega]$

Lowering the resistance gives rise to period three and period four limit cycles; both of them are called tangent bifurcations. These are arguably the most interesting, since they are a strong indication that the experimental setup is capable of generating chaos [6]. Also notable is the fact that there is only a 1 $[\Omega]$ separation between both limit cycles on the numerical prediction (1993 $[\Omega]$ vs 1992 $[\Omega]$), and 8 $[\Omega]$ on the experimental prediction (1677 $[\Omega]$ vs 1669 $[\Omega]$).

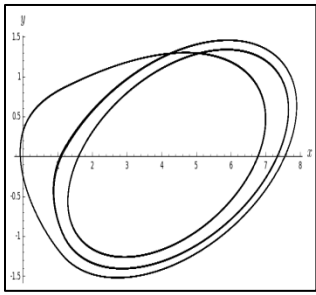


Figure 17- Numerical prediction for the “triple loop” single scroll with periodic window.
R= 1993 [Ω]

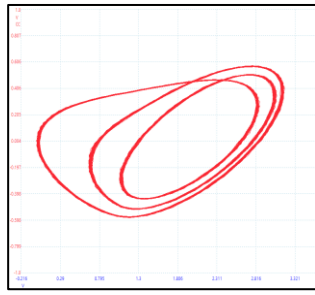


Figure 18- Experimental result for the “triple loop” single scroll with periodic window
R= 1677 [Ω]

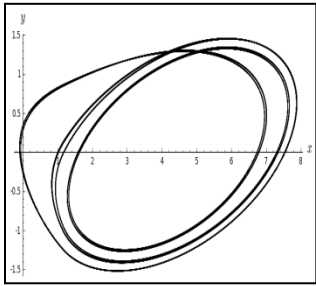


Figure 19- Numerical prediction for the “quadruple loop” single scroll with periodic window.
R= 1992 [Ω]

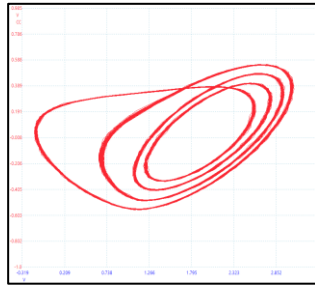


Figure 20- Experimental result for the “quadruple loop” single scroll with periodic window
R= 1669 [Ω]

Chaos appears as these transitions become more and more frequent, making the oscillation essentially aperiodic. The “birth” of the single scroll chaotic attractor was observed at 1974 [Ω] on the numerical prediction and 1650 [Ω] on the experiment.

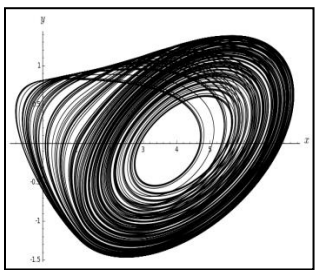


Figure 21- Numerical prediction for a single chaotic scroll.
R= 1974 [Ω]

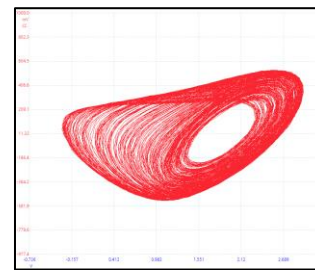


Figure 22- Experimental result for a single chaotic scroll
R= 1650 [Ω]

Apart from weaker dissipation, a reduction of the resistance also moves the outer equilibrium point closer to the center.

With enough reduction, when the trajectory enters the inner region, the real eigenvector is not able to push it back immediately, but instead the curve has the chance of getting over to the other side of the origin, thereby connecting the two possible single scroll solutions into a double scroll [3].

It is clear that the lower the resistance, the more the system behave as one large attractor, with turning to the other side being as likely as staying. The first appearance of the double scroll attractor was observed at 1961 [Ω] on the numerical prediction and 1627 [Ω] on the experiment.

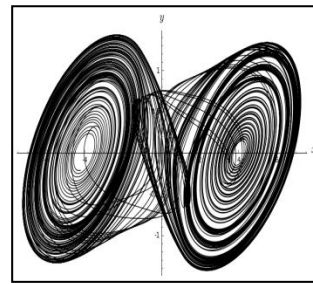


Figure 23- Numerical prediction for a double scroll.
R= 1961 [Ω]

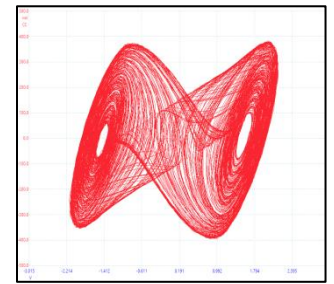


Figure 24- Experimental result for a double scroll
R= 1627 [Ω]

As the resistance keeps being lowered, so does the nature of the double scroll. A “quadruple loop” double scroll with periodic window was observed at 1851 [Ω] on the numerical prediction and 1607 [Ω] on the experiment.

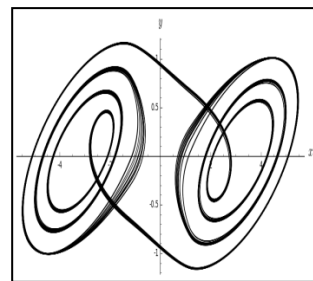


Figure 25- Numerical prediction for the “quadruple loop” double scroll with periodic window.
R= 1851 [Ω]

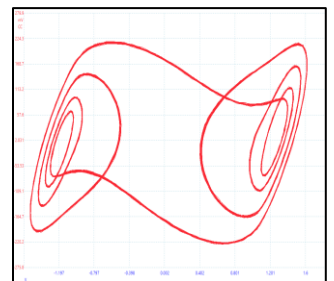


Figure 26- Experimental result for the “quadruple loop” double scroll with periodic window
R= 1607 [Ω]

As the fixed points keep moving towards each other, a point is reached where the center starts becoming too dissipative. This changes the attractor behavior, as the orbit now starts to go from one fixed point to the other one through the outwards, instead of the center.

The homoclinic double scroll was first observed at 1783 [Ω] on the numerical prediction and 1532 [Ω] on the experiment.

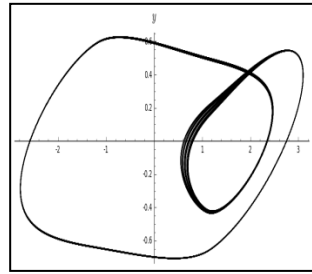


Figure 31- Numerical prediction for another double scroll with periodic window.
R= 1610 [Ω]

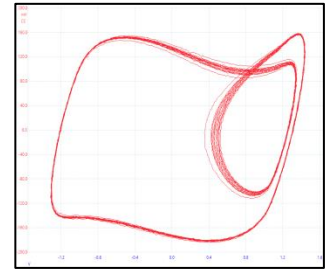


Figure 32- Experimental result for another double scroll with periodic window
R= 1307 [Ω]

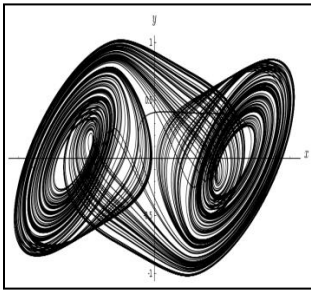


Figure 27- Numerical prediction for an homoclinic double scroll.
R= 1783 [Ω]

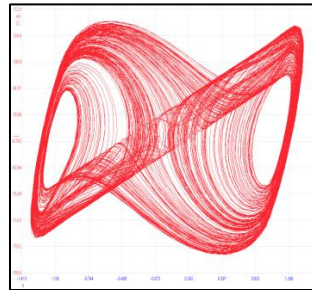


Figure 28- Experimental result for an homoclinic double scroll
R= 1532 [Ω]

The homoclinic double scroll also comes with limit cycles. Figures 29 through 33 explore the ones found on this work.

When the resistance becomes low enough, the outer equilibrium points will come closer and closer to the inner region. For a trajectory rather far away from the three points, they will then effectively behave as a single repulsive point, pushing out the trajectory into the outmost region. This area is strongly dissipative and will, therefore, send the trajectory back, giving rise to a large limit cycle in the outmost region [3].

As the theoretical behaviour for the Chua diode does not agree with experimental measurements due to current limitations (nor are the operational amplifiers built to work in this region), no greater interest was given to this region.

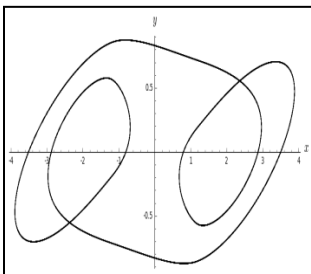


Figure 29- Numerical prediction for the "single loop" double scroll with periodic window.
R= 1706 [Ω]

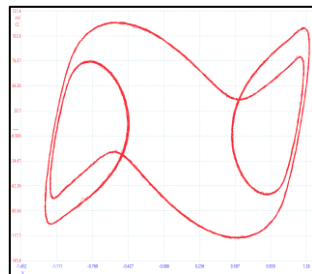


Figure 30- Experimental result for the "single loop" double scroll with periodic window
R= 1427 [Ω]

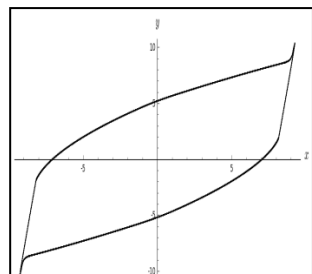


Figure 33- Numerical prediction for the outmost limit cycle.

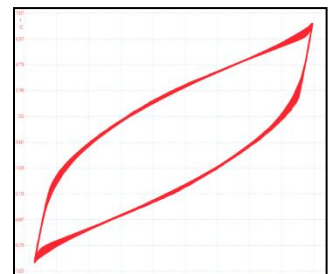


Figure 34- Experimental result for the outmost limit cycle.

6.2 Synchronization of two Chua Circuits via Bidirectional Method

Figures 35 and 36 show how the signals look when the circuits are not synchronized and how they look when it is turned on.

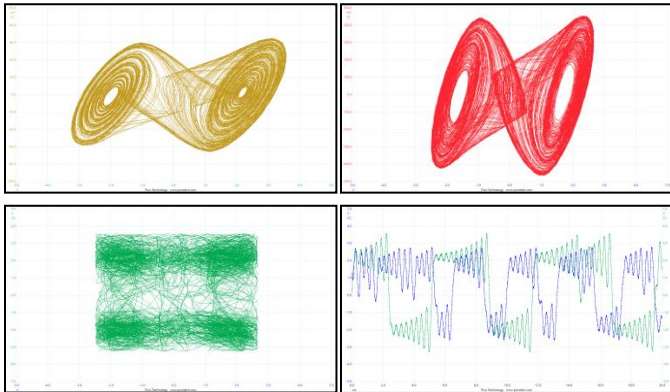


Figure 35- Unsynchronized Chua Circuits.

The upper images on both figures show both of the Chua circuits. The lower left image shows both X coordinates plotted against each other, and the lower right image shows both X coordinates plotted against time.

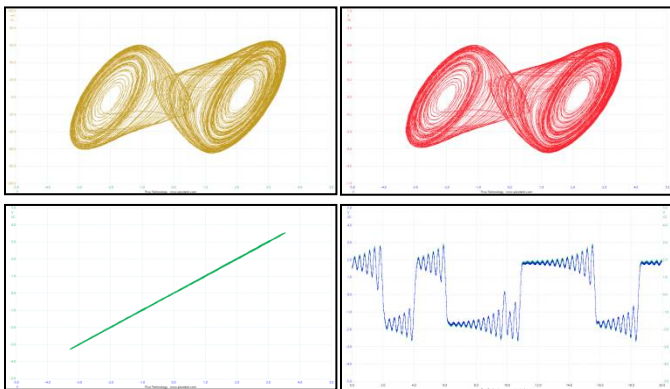


Figure 36- Synchronized Chua Circuits.

7. Discussion

The circuit showed intermittent chaos from 1307Ω to 1777Ω , and were in agreement with the numerical simulation within an 11.81% to 18.81% relative error range.

An explanation for this margin of error is the capacitors. The circuit used capacitors in the order of magnitude of 10 and 100 [nF]. In this range, commercial instruments available at the time of this work had an inaccuracy of at least 10% which added together make the circuit too imprecise to reach a margin of error lesser than 10%.

In the case of bidirectional synchronization the circuits are diffusively coupled using the first state. When the circuits were not synchronized both attractors looks similar, but their time signals were very different. When they were synchronized a 45° angle on the plot of X vs X plot. The signals also perfectly match each other on the plot of X vs time.

Several resistor values were used to attempt synchronization. When the resistor was lowered the coupling strength increased, lowering the synchronization error. The opposite happened for increasing resistor values. If the resistor value is high enough, the coupling is too weak to synchronize the circuits and they operate as free systems.

8. Conclusion

The Chua circuit is a complex system capable of generating bifurcation and chaos phenomena. The nonlinearity of the circuit is given by a piece-wise linear characteristic, which consists of three linear parts. The objective of this work was to analyze its dynamic behavior with an experimental realization of the circuit. To compare the obtained experimental results a numerical setup was also designed. Both the experimental and numerical methods were compared visually and in terms of the bifurcation parameter R.

As a last part of this project, two Chua circuits were synchronized using the bidirectional synchronization method. This last part was successful, as the results coincide with what Strogatz on chapter 9 of this book.

Chaotic synchronization has been receiving increasing in literature since the publication of [9]. Examples of applications of chaotic synchronization can be found in [10]. The bursting phenomenon, which occurs if the coupling strength crosses a certain threshold value, should be investigated further. A possible technique that can be used is the examination of transverse Lyapunov exponents of the synchronization manifold. This is explored on [11].

Previous work [12] has suggested the possibility of extending the synchronization concept to that of a metaphor for some neural processes. It has been suggested that one should view the brain response as an attractor. It has also been further theorized [13] that the process of synchronization can be viewed as a response system that “knows” what state (attractor) to go when driven (stimulated) by a particular signal. Both authors coincide in that this dynamical view could supplant the more “fixed-point” view of neural nets.

Synchronization of chaos has also found application in many areas of physics, biology, and engineering. This is why it is important to continue addressing its issues and exploring the subject.

9. Bibliography

- [1] E. Lorenz, *The essence of chaos*. Seattle: University of Washington Press, 1995.
- [2] L. O. Chua, “Chua’s circuit 10 years later,” *International Journal of Circuit Theory and Applications*, vol. 22, no. 4, pp. 279–305, 1994.
- [3] Jakob Lavröd, “The Anatomy of a Chua Circuit”, *Bachelor Thesis Equivalent to 15 ECTS*. Division of Mathematical Physics. Lunds Universitet.
- [4] K. G. Andersson and L.-C. Böiers, *Ordinära differentialekvationer / Karl Gustav Andersson, Lars-Christer Böiers*. Lund : Studentlitteratur, 1992 ; (Lund : Studentlitteratur), 1992.
- [5] G. Baker, *Chaotic dynamics : an introduction*. Cambridge New York: Cambridge University Press, 1996.
- [6] R. van der Steen, *Numerical and experimental analysis of multiple Chua circuits*. Eindhoven University of Technology, 2006.
- [7] Leonov, G.A., D.V. Ponomarenko and V.B. Smirnova, *Frequency methods for nonlinear analysis*. Theory and applications. World Scientific. Singapore, 1996.
- [8] M. P. Kennedy, “Robust op amp realization of chua’s circuit,” *Frequenz*, vol. 46, pp. 66–80, 1992.
- [9] Pecora, L.M. and T.L. Carroll, *Synchronization in chaotic systems*. *Physical Review Letters* 64(8), 821–824. 1990.
- [10] Dedieu, H., M.P. Kennedy and M. Hasler, *Chaos shift keying: Modulation and demodulation of a chaotic carrier using self-synchronizing Chua’s circuits*. *IEEE Transactions on Circuits and Systems II* 40(10), 634–642. 1993.
- [11] Heagy, J.F., T.L. Carroll and L.M. Pecora. *Synchronous chaos in coupled oscillator systems*. *Physical Review E* 50(3), 1874–1886. 1994
- [12] Christine A. Skarda & Walter J. Freeman. *How brains make chaos in order to make sense of the world*. *Behavioral and Brain Sciences* 10. 1987
- [13] Garfinkel A. *A mathematics for physiology*. *Am J Physiol*. 1983